

ON THE DELAY OF THE ADDITIONAL MORTALITY LINKED TO THE GEOMAGNETIC DISTURBANCES

Tsvetan Georgiev, Siyka Simeonova, Luba Dankova

*Institute of Astronomy and National Astronomical Observatory –
Bulgarian Academy of Sciences
e-mail: tsgeorg@astro.bas.bg*

Keywords: *Geomagnetic disturbances, Sun- mortality relationship*

Abstract

The geomagnetic disturbances, mainly geomagnetic storms (GMSs), but also low frequency resonances, touch some people susceptible to cerebrovascular diseases (CVDs). Sometimes the geomagnetic effect is overestimating speculatively. Against this concept we compare the changes of geomagnetic indexes (GMIs) with the changes of additional mortality rate (AMR). We compare by means of cross-correlation functions (CCFs) and use the Wolf number (WN) as referent time scale. We suspect that strong GMSs, like these in 2003, increase the relative common MR 3–4 years later with up to 4×10^{-5} . Otherwise, the typical GMS linked AMR seems to be less than 10^{-5} . Even if these our values are overestimated, generally they are small. Analyzing data about Bulgaria and 5 its regions for the last Solar cycles, we confirm that the lag of the maxima of the GMS linked ANR behind the WN maxima is ~ 5 years. We confirm also that the lag of the GMSs maxima behind the WN maximum is 1–2 years. Especially, we found that the lag of the maxima of the CVD linked AMR behind the maxima of the GMSs is 3–4 years. So, we consider the 5 years lag of the AMR linked to the GMSs behind the WN maximum appears a sum of two above mentioned delays, 1–2 years and 3–4 years. In principle, the typical duration of CVDs may be derived if the beginnings are known. In the medicine they are usually unknown. However, suspecting the GMSs as triggers of a part of the CWD linked AMR, we should suppose that these CWDs finish with lethal outcome after 3–4 years.

Introduction

Usually, the moments of the geomagnetic activity are referred to the time scale of the Wolf number (WN). The WN W is defined as a relative number of the sunspots. The number and the intensities of the high energetic solar processes, which affect the Earth, correlate with the WN.

The changes of the speed and density of the solar wind (due to the flares and coronal mass ejections) cause geomagnetic disturbances (GMDs) with a duration up to several hours. The GMDs, especially the geomagnetic storms (GMSs), affect many processes on Earth, including somewhat the human health. The GMDs are characterized by geomagnetic indexes (GMIs, Section 2). The GMS

maxima lag behind WN maxima by 1–2 years ([1], Figs. 17, 19; [2], Figs. 5, 6; [3], Fig. 1; [4], Fig. 3). In this work the lag of the GMS maxima behind the WN maxima is found to be also 1–2 years. See our Figs. 4 right, 6.

The proton concentration N_p above the Earth atmosphere is due mainly to the galactic cosmic rays, varies. While the solar activity is high, the solar wind suppresses the galactic cosmic rays and N_p is low (effect of Forbush). When N_p is high and variable, it creates low-frequency electromagnetic resonances (LFRs) in the chamber between the Earth surface and the ionosphere (Schumann resonances). When the resonance frequency is very low, 1–2 Hz, it may be somewhat dangerous for the heart rhythm of some people [5, 6]. The LFR maxima lag behind the WN maxima, depending on the solar wind intensity, is 4–7 years. It takes place over and after the WN minima. See our Figs. 2a, 6d.

The GMDs are linked to some health outcomes, connected mainly to the cerebrovascular diseases (CVDs) – coronary heart diseases, myocardial infarction (MI), brain stroke (BS), etc. The GMDs are linking also to neurological system diseases, behavioral diseases, etc. In principle, the CVDs are the cause for a half of the common mortality rate (MR) worldwide. However, in this paper we concentrate on the additional MR (AMR), caused suggestively by the GMDs.

Usually, the studies are concentrated on the correlation of solar activity and MIs and/or BSs. Many evidences exist about the negative influence of the GMDs and LFRs on the physiological and psychological human health, [7–10]. For example, during days with GMS the additional BSs and MIs suffers in Moscow grow by 7.5% and 13%, respectively. (See the references of the Russian studies in [11]). It is established also that the GMDs, caused by solar magnetic clouds, are related to increase of MI. The last mentioned connection is higher in comparison with the GMDs caused by high speed solar wind streams and in days with quiet geomagnetic activity, [12].

Ionosphere and geomagnetic changes influence on mortality from circulatory diseases. The CVDs response to the changes in the solar activity and to abnormal solar events influence indirectly the concentration of electrical charges in the Earth's environment, [13]. The different patterns in daily numbers of deaths during the quiet periods of solar activity are examined later. It is shown that there are a connection between the daily number of deaths and all indices of solar and geomagnetic activity in periods of low solar activity, in contrast to periods of strong solar storms, [14].

The relationships between GMDs and the time course and lags of autonomic nervous system responses have been examined in [14]. It is confirmed that the daily nervous system activity responds to GMDs. The response is initiated at different times after the changes in the various environmental factors and persists over varying time periods. Increase in solar wind, cosmic rays, solar radio flux, and Schumann resonance power was all associated with increased heart rate and parasympathetic activity, which is interpret as a biological stress response. The

people are affected different ways depending on their sensitivity, health status and capacity for self regulation. The impact of short exposure to GMDs on total and cause-specific MR in 263 US cities is investigated recently, [3]. The GMDs and LFRs lead to an increase in city-specific and season-stratified common MR in all cities. The effects on total deaths were found in all seasons, and on CVD and MI deaths – more in spring and autumn. These results may be explain through the direct impact of environmental electric and magnetic fields produced during GMDs and LFRs on the human autonomic nervous system.

In a review on health effects of the GMDs, Palmer et al. (2006), [16], reported 5 definite conclusions: (1) GMDs have a greater effect on humans at higher geomagnetic latitudes. (2) Unusually high geomagnetic activity seems to have a negative effect on human cardiovascular health. (3) Unusually low values of geomagnetic activity seem to have a negative effect on human health. (4) Only 10–15% of the people are negatively affected by GMDs and (5) heart rhythm variations are negatively correlated with GMD. In this paper, we confirm that the lag of the AMR maxima behind the maxima of the WN is about 5 years (see our Figs. 2). We propose an explanation of this “paradox”. See our Summary.

Earlier, we found correlations of the an cause-specific CVD AMR linked with GMSs for Smlyan region of Bulgaria [11]. We found that with respect to the years with low CMDs (1993, 1995, 1996, 1999), in the years with strong GMSs (2000, 2001, 2003–2005), the AMR is higher with 20–30% and the MR related to CVD is higher with 30–40% ([11], Figs.10–13). We noted also that the time delay of the maximum of the common and CVD AMRs in 2007–2008 takes place about 3–4 years behind the maximum of the strong storms in 2003–2005 (see Fig. 1a). The increasing in AMR and in common MR is about 50% and 5%, respectively. This result leads to the suggestion that the influence of the GMSs on the AMR may manifests itself 3–4 years later. This is the motivation of the present work.

In this paper, time delays of the AMR maxima are revealed by maxima positions of cross-correlation functions (CCFs). The CCF is a measure of the similarity between the structures of two time series. It is a function of their relative lag time t_L (Fig. 2, 3). The large scale trend in the series is obstacle and it must be removed preliminary. Fortunately, all time series used here pose linear large scale trends. For example, in Fig. 2 we juxtapose the WN, W , and a few kinds of MR, M , after removal of their linear fits. Thus the CCF uses the deviations, for example $\Delta W = W - W_F$ and $\Delta M = M - M_F$, where W_F and M_F are the relevant linear fits of the time series. The deviation ΔM is just the AMR.

So, in this work, the maxima positions of the CCFs are used for determination of time lags of the time series Θ (Figs.6–11). The CCF maximum is characterized by its value C and its standard error σ_C . The CCF maxima in thus paper are not high, often about 0.6, but their standard errors are relatively small. Then, the Student ratio $R=C/\sigma_C$ is usually high, giving evidence that the CCF maxima are significant. (Figs. 4–11).

Note that a graphical representation of the Student criterion for such cases in [17], Fig. 4, show easy how the threshold increases when the data number decreases. So, 20–10 data the 95% threshold is 0.6–1.1 and the 99% threshold is 0.9–1.6. Sometimes our ratio R overcomes the threshold. Note also that the GMSs, LFRs and CVDs have very complicated origin and nature, which is out of the subject of this work. We are interested mainly on the cross-correlations between the deviations from the GMI fits (reasons) and the deviations from the MR fits (results), regarded as AMR.

Used abbreviations follow.

AMR – additional mortality rate;

BS – brain stroke;

CCF – cross-correlation function;

CVD – cerebrovascular disease;

GMD – geomagnetic disturbance;

GMI – geomagnetic index;

GM – geomagnetic storm;

LFR – low-frequency resonance;

MI – myocardial infarction;

MR – mortality rate;

NI – NASA (planetary) indexes (Section 2: B , Kp , Ap , Np ; Figs. 5, 6);

PI – Panagyurishte (local) indexes (Section 2: Sa , Sb , Sc , Sn ; Fig. 4);

WN – Wolf number of the sunspots.

1. Data about the MR. Lags of the ANRs behind the WNs.

Figure 1 shows the behaviour of the habitant numbers N (circles) and MRM (dots) over years. The numbers N are expressed in specific (implemented) units. The numbers M are expressed always per mile (in $10^{-3} N$). Hereafter the straight lines show the fits while g and s are gradient (slope coefficient) and standard deviation of the fit.

Figure 1a shows the initial data about Smolyan region, Rodopi Mountain, in 1988–2008 yr [11] (Sun cycles 22+23). These data are valuable here, because only they contain the common MR M_1 , as well as the medically confirmed CVD MR M_0 . The data content follow:

N_1 – habitant number;

M_1 – common MR;

M_0 – MR linked medically with CVD;

M_D – residual MR, $M_D = M_1 - M_0$.

The residual MR M_D corresponds deaths caused by other reasons, including LFRs.

In the time episode of Fig.1a N_1 decreases 1.3 fold, mainly by migration of young people. Simultaneously, M_1 increases 1.5 fold, mainly because the population gets older. The increases of M_0 and M_D are about 1.4 and 1.3 fold,

respectively. In Fig.1a two squares show extraordinary maximum of the CVD MR M_0 . Two large dots show respective deep minima in the residual mortality M_D . (The data marked by squares and dots do not participate in the relevant fits.)

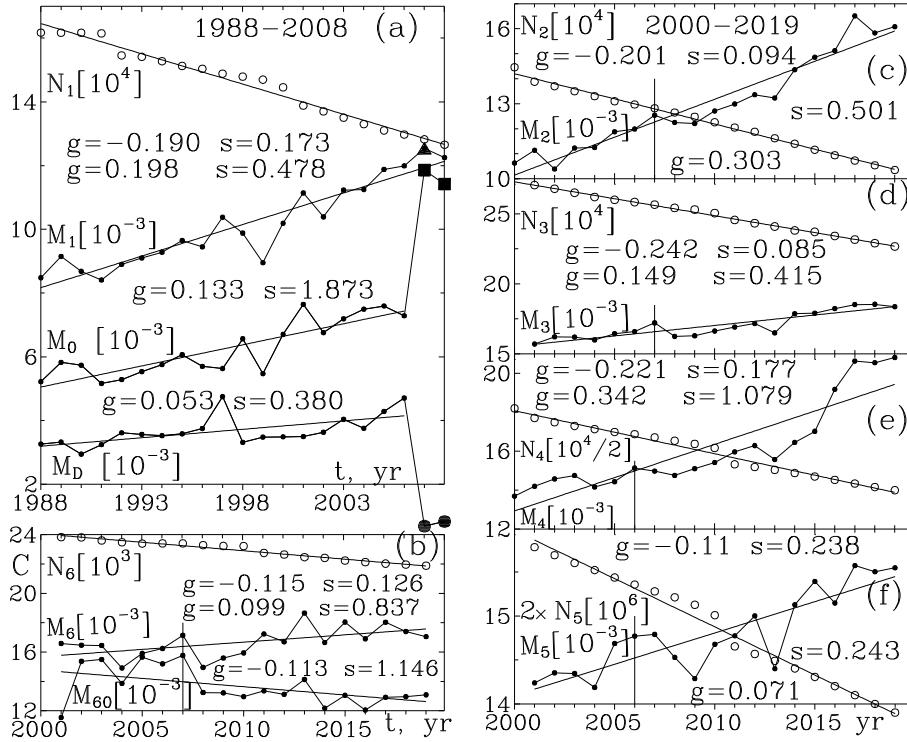


Fig. 1. Annual data about the habitants N and mortalities M for 5 Bulgarian regions plus Bulgaria as a whole. See the text in the beginning of Section 1.

Figures 1b–1f show 5 MR data systems for the time episode 2000–2019 yr (Sun cycles are 23+24). The source of data is the National Statistical Institute of Bulgaria [18]. The data content follow:

- N_2, M_2 – again for Smolyan region, Fig. 1c;
- N_3, M_3 – for Sofia suburb (without Sofia city), Fig. 1d;
- N_4, M_4 – for region of Dobrich plus Silistra together, Fig. 1e;
- N_5, M_5 – for Bulgaria as a whole, Fig. 1f;
- N_6, M_6, M_{60} -- for eastern part of the Sofia suburb, Fig. 1b.

In the time episode of Figs. 1b–1f all habitant numbers N_2 – N_6 decrease and all common MRs M_2 – M_6 increase. The reason is the same as in Fig. 1a. The region in Fig. 1b (namely Elin Pelin) covers about 1/10 of the habitants of the Sofia suburb, but it is also valuable here. It contains two kinds of common MR. M_{60} is

recorded only inside the territory of this region and it decreases. M_6 is the common MR, containing M_{60} plus number of deaths of habitants of this region, but recorded in the nearby big hospital in Sofia. As it is expected, M_6 increases.

Let us a return to Fig. 1. There we may estimate the extremely and the ordinary AMR, linked with the GMS. The extraordinary CVD MR M_0 in 2006–2007, after the strong GMSs in 2003, exceeds the local MR M_0 by $\sim 50\%$ (Fig. 1a). The relevant small peak in the common M_1 exceeds the local MR M_1 with $\sim 4\%$. The vertical segments in Figs. 1b–1f mark the respective small local peaks of the common MR in 2006–2007 yr. The height of these peaks, including for Bulgaria as a hole, is up to $\sim 4\%$ above the local MR.

So, the strong GMSs (in this single case) seems trigger for increase of the common MR up to $\sim \Delta M = 0.04 \times 10^{-5} = 4 \times 10^{-5}$, with a time lag of 3–4 yr. Otherwise, the typical CVD AMR, linked with GMSs, seems to be up to 1×10^{-5} per year. Because of unknown random AMR contributions, these AMR seems to be overestimated, tough. These AMR values seems to be neglect. For comparison, the deaths by car accidents for Bulgaria as whole, in 2017, is $\sim 10 \times 10^{-5}$. Both values are overestimated and need of justification.

The deviations of the MRs from the linear fits in Fig. 1a, ΔM_1 , ΔM_0 or ΔM_D , are the AMR. After fit removal these deviations participate in 3 important CCFs in Fig. 2a. They distinct the supposed contributions of CVD linked MR, common MR and common MR minus CVD linked NR LFR MR. The deviations of the MRs ΔM_1 – ΔM_5 show clearly the delay of the AMR linked with the GMDs in respect with the WN maxima.

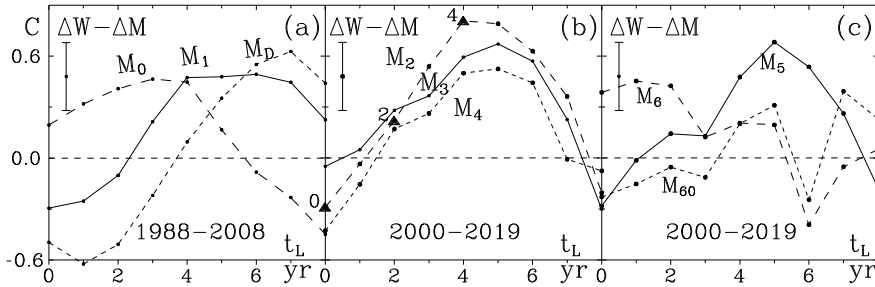


Fig. 2. CCFs between the changes of the WNs and fluctuations of the AMRs. The maxima position show the delay of the AMR. See the text in Section 1.

Figure 2 juxtaposes CCFs $C(t_L)$ between the WNs (shown in Fig. 5) and AMRs (shown in Fig. 1) over the time lag t_L . The CCF maxima mark the time lag of the AMR maxima behind the WN maxima. Note, that linear fits of the compared time series are removed always. Vertical segments show the typical error bars of the CCF values. Triangles in (b) mark the CCF values whose value deriving are illustrated in Fig. 3. Details about these graphs are shown in Figs. 7–11.

Figure 2a shows the CCFs of WNs with the data M_1 , M_0 , and M_D from Fig. 1a. The CCFs have similar shapes. They show maxima lags behind the WNs of 3, 5 and 7 yr, respectively. The middle maximum, at about 5 yr, corresponds to the common AMR. However, the maxima at 3 and 7 yr may be linked to displays of CVD AMRs, as well as of LFR AMRs. In both cases some additions of deaths by other reasons are present undoubtedly.

Figure 2b shows the CCFs for the data M_2 , M_3 , and M_4 in Fig. 1c–1e. The CCFs have again similar shapes. Their maxima show lags behind the WN about 5 yr. Hints of humps in the left parts of the CCFs, about lag of 2 yr, seem linked with CVD AMR. Triangles mark the CCF values whose deriving as coefficient of correlation are illustrated in Fig. 3.

Figure 2c shows by solid lines the CCF for the AMR of Bulgaria as a whole, M_5 from Fig. 1c. The shape is similar to mentioned shapes of CCFs, with peak lag of 5 yr behind the WN. This CCF shows a local convexity at a lag of about 2 yr, which ought to be linked with contribution of CVD AMR. Figure 2c shows by dashed broken lines the CCFs for the common AMRs M_6 and the territory bounded AMR M_{60} . These curves are very different. The left part of CCF for M_{60} is flat as if CVD AMRs are missing. Obviously, significant number of CVS AMP happen out of the territory, in the nearby big hospital. Remarkable hump is present of the left part of the CCF only in the common AMR M_6 . It seems CVD AMR dominates in this region.

In Fig. 2 the humps at lags of about 5 yr behind the WRs contain contributions from the CVD, LFR and other AMRs. It may be seen well in M_0 , Fig. 2a, with lag 2–4 yr. In the other cases suspected, in M_2 – M_5 with lag of about 2 yr and in M_6 with lag of 1–2 yr.

So, if the strong GMDs are regarded as triggers of a part of the CVDs, with postponed lethal outcome, then the lags of the GMD AMR behind the WNs, as well the lags of AMRs behind the GMDs, may be revealed. In Section 2, we derive lags of GMIs behind the WNs. In Section 3, we show details of deriving of the CCFs shown in Fig. 2.

Figure 3 shows the derivations of the CCF values at t_L -lags of 0, 2 and 4 yr, marked in Fig. 2b by triangles. Top panels show the shifts of the shape of the WNs (thick broken lines) over the shape of AMR (thin broken lines). Linear fits of the compared series are removed. Here n is the number of currently used points. Dashed broken lines show the useless edges of the time series after the shifts of WNs. Bottom panels show the respective correlation diagrams and CCF values C . Solid and dashed lines represent direct and reverse linear fits. Note that because of the large range of the WN, the compatibility of the graphs in the top panels is difficult. By this reason the WN values $W=W^{0.5}/20$ are used. This is admissible because the values of the CCFs are dimensionless. Note that the values of C in the case (c_2), after suitable mutual shift, becomes significant.

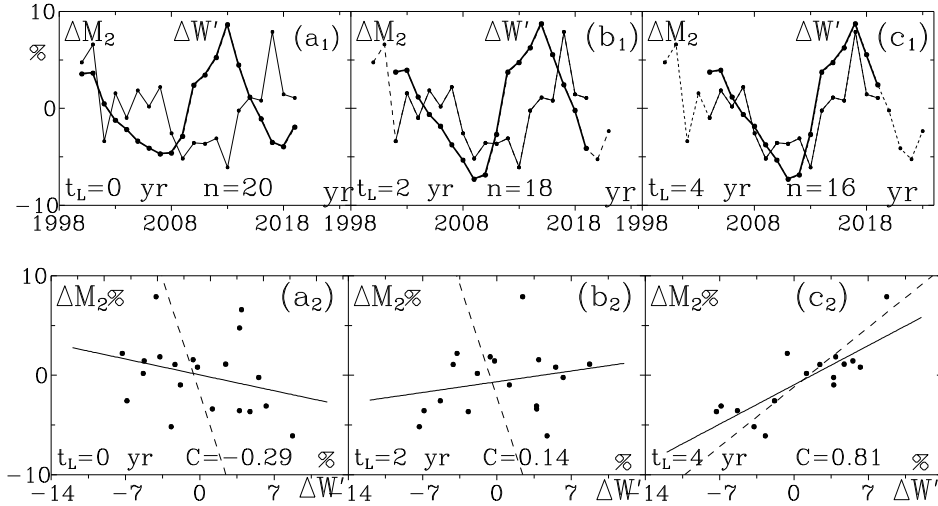


Fig. 3. illustrates the action of the CCF and the sources of the CCF values at points 0, 2 and 4 in Fig. 2b

2. Indexes about the GMDs. Lags of the GMDs behind the WNs

Initially, local GMI in 1988-2008 are acquired from the Panagyurishte Geomagnetic Observatory of Bulgaria [11]. The Panagyurishte indexes (PIs) used here are derivatives of the measured vertical component H of the local geomagnetic field. The used annual PIs are:

- Sa – average amplitude of all storms, in nT;
- Sb – average amplitude of the moderate and strong storms, for $H > 120$ nT;
- Sc – average amplitude of Sb -type storms, but with sudden onset, in nT;
- Sn – number of all storms.

Figure 4 show the behaviour of the PIs and their CCF with WNs. Figure 4, left graphs, represents the behaviour of the PIs and their trends over years. Hereafter g and s are the gradient and the standard error of the fits. The graphs cover the Sun cycles 22+23. In this episode the common solar activity decreases (see Figs. 4d₁, 5a₁–5e₁), but the large scale trends of Sa and Sb are slightly positive. The powerful GMSs in 2003–2005 cause high peaks in the graphs of Sa – Sc . Figure 4, right graphs, show the CCFs $C(t_L)$ of the PIs with the WNs over the time lag t_L . Hereafter θ and C are the delay and the value of the CCF maximum. $R = C/\sigma_C$ is the Student ratio. The CCF maxima are relatively low and blunt. The time lags θ of the CCFs maxima behind the WN maximum are 2, 1, 2, and 0 yr, respectively. Note, that the number of all GMSs Sn reflects the general decrease of the solar activity and obeys the behaviour of the WN trend (Fig. 4d₁, 4d₂). The PI Sn occurs

useless in the study of the AMR delays. Therefore, we may consider the lag of the GMSs behind the WN maxima to be roughly 2 years.

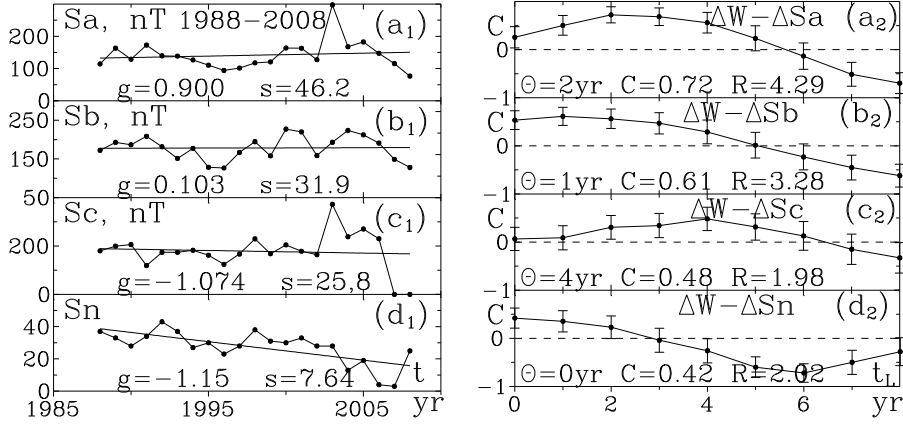


Fig. 4. PIs in Solar cycles 22+23 and their CCFs with the WNs. See the text.

We use also GMIs for 1988–2008 and 2000–2019 from the NASA website [19]. The NASA (planetary) annual indexes (NIs) used here are:

W – Wolf number of the sunspots;

Bm – scalar value of the Earth magnetic field, in nT;

Kp – GMI that characterizes the fluctuations of the electromagnetic field due to the GMSs;

Ap – GMI like Kp and approximately proportional to $\log Kp$;

Np – proton concentration above the Earth atmosphere, in cm^{-1} .

The NIs Kp and Ap indicate indirectly the powers of the GMSs. See [20].

Figure 5 represents the behaviour of the NIs and their trends over years 1988–2008 (cycles 22+23, left graphs) and over 1998–2019 (cycles 23+24, right graphs). The right graphs show that the decrease of the common solar activity goes on, but with decreasing Np in Fig. 5d₂ even increases weakly. The power storms in 2003 are observed as peaks in Kp and Ap .

Figure 6 shows the CCFs of the NIs and the WNs. The CCFs pose again blunt maxima. The lags Θ of the NIs behind the WNs are 0, 0, 0, 6 years in the left graphs and 1, 2, 2, 4 years in the right graphs. The lags of the NIs Bm , Kp and Ap behind the WNs in both cases may be consider to be 0–1 yr or 1–3 yr. Further, the contributions of the AMRs, linked to different GMIs, will be regard separately.

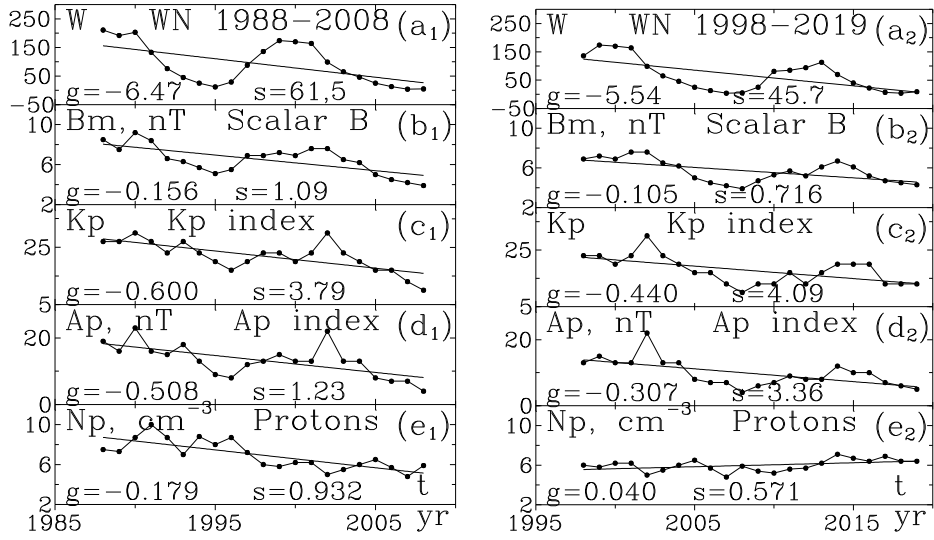


Fig. 5. NIs in Solar cycles 22+23 (left graphs) and 23+24 (rightt graphs).
See Fig. 4, left graph, and the text.

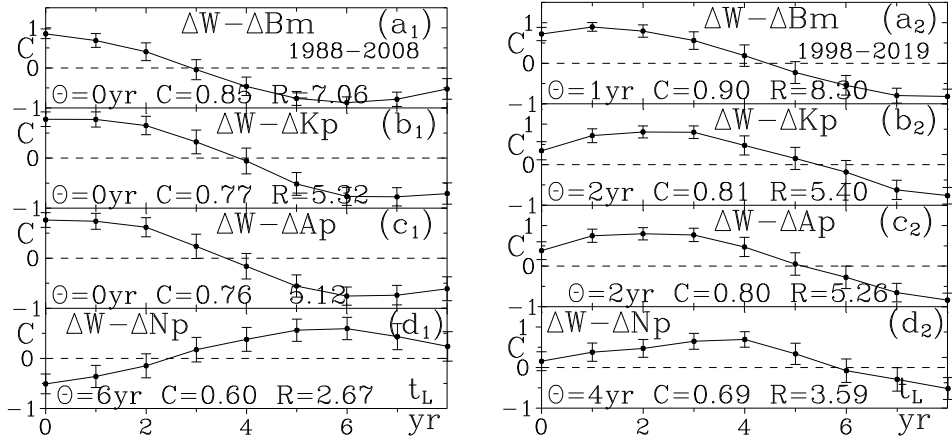


Fig. 6. CCFs between NIs and the WNs for 1988–2008 (left graphs) and for 1998–2019. See also Fig. 4, right graphs and the text.

The proton concentration Np is very interesting. Its maxima lags in Figs. 6d₁ or Fig.6d₂ behind the WN are 5–7 yr or 3–4 yr, respectively. In Fig. 6d₁ this is effect higher solar activity (and higher Forbush effect). Then the LFR linked AMR contribution is distinct, as in Fig. 2a. In Fig. 6d₂ this is effect lower solar activity (and lower Forbush effect). Then the LFR linked AMR contributes to the ordinary

CCF maxima in Fig. 2a–2c, i. e. in the region of WN minima. By this reason, the maximum in M_2 in Fig. 2b is higher than the maximum in M_1 in Fig. 2a.

3. Lags of the AMRs behind the GMIs. Explanation of Fig. 2.

Figures 7a–7d show the CCFs between the common AMR M_1 and 4 GMIs for 1988–2006. The lags Θ of the AMR maxima are 4, 3, 0, 5 yr (left graphs with PIs) or 5, 5, 5, 2 yr (right graphs with NIs). Figures 7e₁ and 7e₂ show the CCF between M_1 and WN (thick broken curve), as in Fig. 2a. Here the beginning parts of the CCFs in (a)–(d) (thin dashed broken curves) are implemented. Note, that the added curves are shifted to the right in accordance to their specific lags behind the GMI maxima in Figs. 4b and 6a. So, the systems of added curves describe approximately the hump of the "main" CCFs (thick broken curves), better in 7e₂. The maximum of the common AMR is situated at ~5 yr behind the WN's maximum.

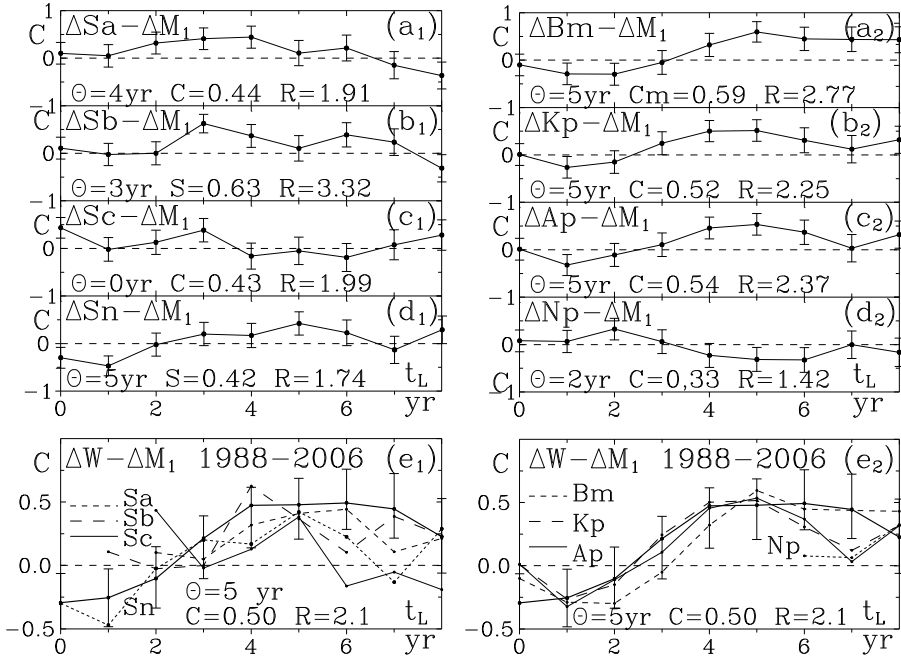


Fig. 7. CCFs for the common AMRs M_1 in Fig. 1a, with PIs (left graphs), NIs (right graphs) and WN (bottom graphs). See Fig. 4, right graphs and text.

Figures 8a–8d show the CCFs between the CVD linked AMR M_0 and 4 GMIs for 1988–2006. The lags Θ of the maxima are 0, 0, 0, 3 yr (left graphs, with PIs) or 3, 2, 2 and 7 (right graphs with NIs). Figures 8e₁ and 8e₂ show the CCFs

between M_{10} and WN (thick broken curves), as in Fig. 2a. Similar to Figs. 7, the shifted beginning parts of the CCFs in (a)–(d) are implemented in (e) (thin and dashed broken curves). The systems of added curves again describe approximately the hump of the "main" CCFs (thick broken curves), better in 8e₂. The maximum of the CVD linked AMR is situated at ~ 3 yr behind the WNs maximum. It seems, this hump contains significant contribution from CVD linked AMRs.

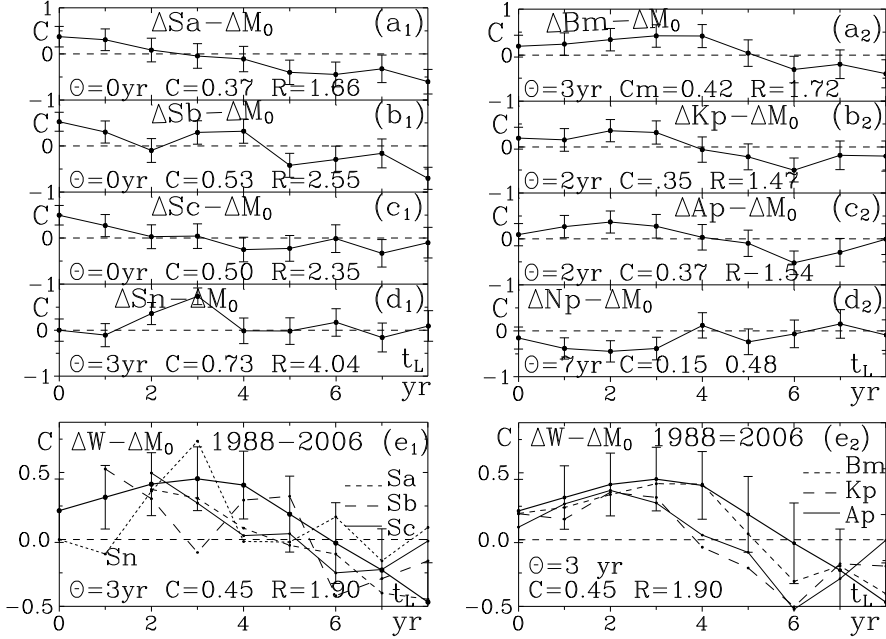


Fig. 8. CCFs for the CVD linked AMRs M_0 in Fig. 1a, with PIs (left graphs), NIs (right graphs) and WN (bottom graphs). See Fig. 4, right graphs and text.

Figures 9a–9d show the CCFs between the residual AMR M_D in Fig. 1a and four GMIs for 1988–2006. The lags Θ of the maxima are 3, 6, 3, 5 yr (left graphs) or 6, 4, 6, 7 (right graphs). Figures 9e₁ and 9e₂ show the CCFs between M_D and WN (thick broken curves), as in Fig. 2a. Similar to Figs. 7 and 8, the shifted beginning parts of the CCFs in (a)–(d) are implemented (thin and dashed broken curves). Again the systems of shifted AMRs describe approximately the position of the hump in the “main” CCFs (thick broken curves), better in (e₂). The maximum of the LFR linked AMR is situated at ~ 7 yr behind the WNs maximum. It seems, this hump contains a significant contribution from LFR linked AMRs.

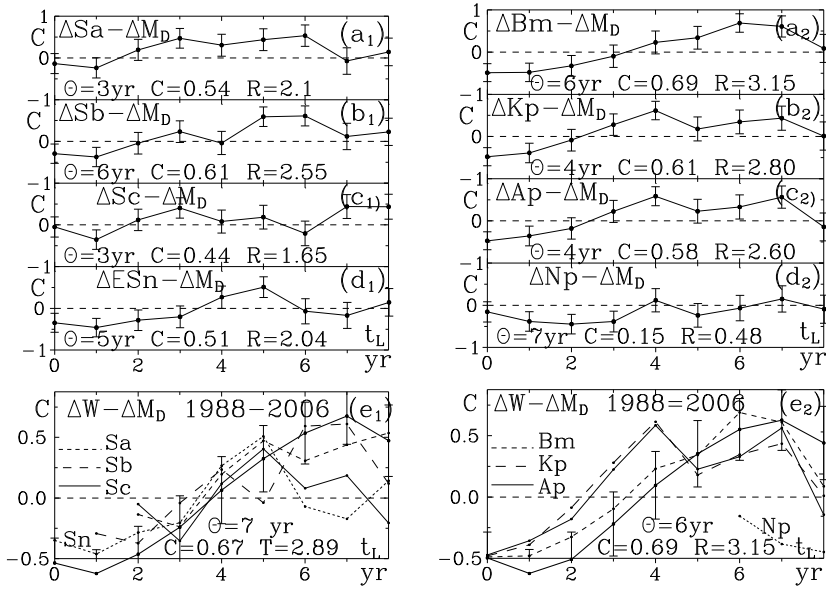


Fig. 9. CCFs for the LFR linked AMRs M_0 in Fig. 1a, with PIs (left graphs), NIs (right graphs) and WN (bottom graphs). See Fig. 4, right graphs and text.

Figures 10 show the CCFs between the common AMRs M_2 and M_3 with 4 NIs for 2000–2018. The lags Θ of the maxima behind the WN maxima is 3, 3, 3, 2 (left graphs) and 3, 1, 3, 2 (right graphs). The typical lag is ~ 3 yr. Again the graphs in 10a–10d are implemented in 10e, shifted in respect to the lags behind their NIs in Fig. 6b. Obviously, the systems of added curves describe well the hump of the "main" CCFs (thick broken curves). The maxima of the common AMRs in Figs. 10e are situated at 4–5 yr behind the WN maximum.

Figures 11 show the CCFs between the common AMR M_4 and M_5 with four NIs for 2000–2018. The lags Θ of the maxima are 4, 3, 3, 2 (left graphs) and 4, 4, 3, 2 (right graphs). The typical lag is ~ 3 yr. Again the graphs in 11a–11d are implemented in 11e, shifted in respect to the lags behind their NIs in Fig. 6b. Obviously, the systems of added curves describe well the hump of the "main" CCFs (thick broken curves). The maximum of the common AMRs is situated at about 5 yr behind the WN maximum.

The humps of the CCFs in Figs. 7e–11e1 which are explained here, are shown together in Fig. ~2. These examples show that the lag of the AMR is about 5 yr behind the maximum of the WN. Simultaneously, this lag may be regarded as a sum of 2 lags: 1–2 yr lag of PI or NI in respect to WN plus 3–4 yr lag of the CVD linked AMR behind the CMIs. Hypothesis appears that the GMDs may be triggers of a part of the CVDs with a postponed lethal outcomes.

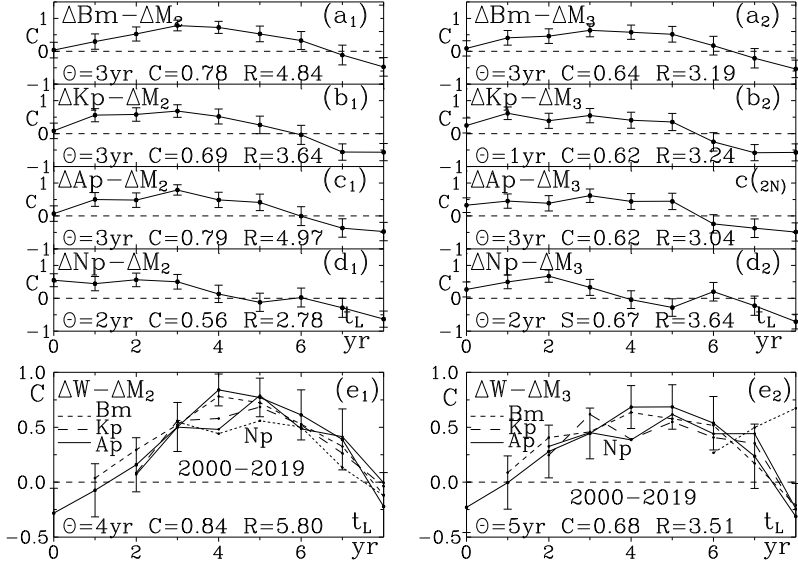


Fig. 10. CCFs for the common AMRs M_2 and M_3 in Fig. 1b, with NIs (left and right graphs), NI and WN (bottom graphs). See Fig. 6, right graphs and text.

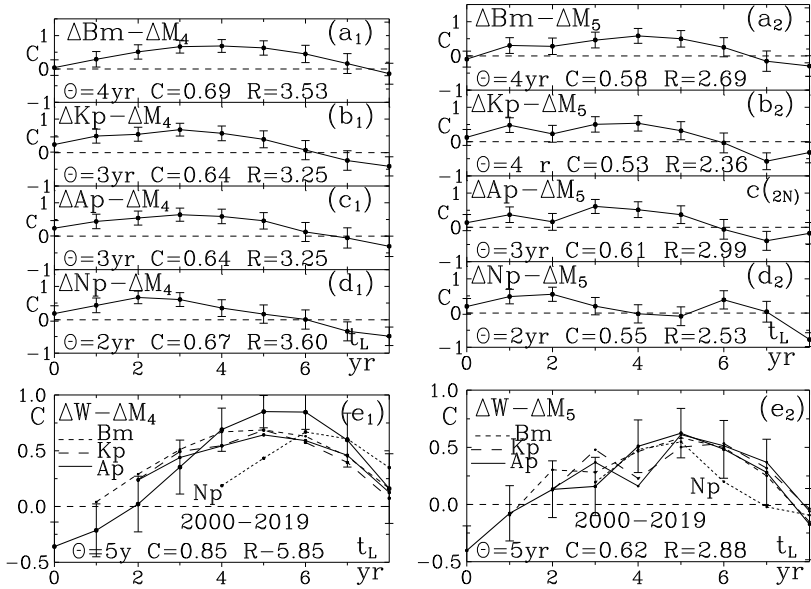


Fig. 11. CCFs for the common AMRs M_4 and M_5 in Fig. 1b and 1c, with NIs (left and right graphs) and WN (bottom graphs). See Fig. 6, right graphs and text.

4. Summary

The main results follow.

1. We confirm our suggest in [11] that the strong GMSs about 2003 yr cause 3–4 year later, in 2006–2007, annual increase of the CVD linked AMR with ~50% (Fig. 1a). The local increase in the common MRs is ~4% (Figs.1b–1f). Therefore, the strongest GMS may increase the common MR by about 4×10^{-5} with a lag of 3–4 yr. Otherwise, the typical CVD linked AMR seems to be up to 10^{-5} .

2. On the base of common AMR data M_1 – M_5 , for five region, including Bulgaria as a whole, we show that the shapes of the CCFs between WN and common AMR are very similar (Fig. 2). The lag of the maxima behind the WN maxima is about 5 years. So, the common AMR maxima fall on the WN minima, confirming the consideration No.3 in [16] (see introduction).

3. We confirm that the lag of the GMSs maxima behind the WN maxima is 1–2 yr (Figs. 4b, 6). We find also that the lag of the CVD ANR maxima or LFR AMR maxima behind the WN maxima is 3–4 yr or 4–7 yr, respectively (Figs. 2; 7–9). Therefore, consider the lag of the maxima of the common ANR behind the WN maxima, typically 5 yr, may be explain as a sum of the above mentioned lags of 1–2 and 3–4 yr.

4. Considering GMSs as triggers for CVDs we estimate that the lasting of the CVDs before the letal outcome is typically 3–4 yr. In the medicine the begins CVDs are not known and such direct estimation is impossible.

Acknowledgements

The author is grateful to Dr. B. Komitov for his attention and recommendations to this work.

References

1. Hathaway, D. H., (2010), Reviews in Solar Physics, Volume 7, The Solar Cycle (Springer).
2. Zerbo, J.-L., C. Amory-mazaudier, F. Ouattara, (2013), Adv. Res. 4/3, 265–274.
3. Zili Vieira, C. L., D. Alvares, A. Blomberg, et al., (2019), Environmental Health 18, No. 8 3.
4. Abe, O. E., M. O. Fakomiti., W. N. Igboama, et al., (2023), Adv. Sp. Res. 71, 2240–2251.
5. Southwood, D., (1974), Planet. Sp. Sci. 22, 483–491.
6. Thayer, J. F., A. L. Hansen, E. Saus-Rose, et al., (2009) Ann. Behav. Med. 37, 141–153.
7. Friedman, H., R. O. Becker, C. H. Bachman, (1967), Nature 213, 949.
8. Gnevyshev, M. N., K. F. Novikova, (1972), J. Interdiscipl. Cycle Res. 3, 99.
9. Lipa, B. J, P. A. Sturrock, E. Rogot, (1976), Nature 259, 302.

10. Malin, S.R., C. Malin., B. J. Srivastava, (1979), Nature, 277, 646
11. Simeonova, S. G., R. C. Georgieva., B. H. Dimitrova, et al., (2010), Bulg. Astron. J. 14, 144–161
12. Dimitrova, S., I. Stoilova, K. Georgieva., et al., (2009), Fund. Sp. Res., HELIOBIOLOGY 161–165
13. Podolská, K., (2018), Journal of Stroke and Cerebrovascular Diseases} 27/2, 404–427.
14. Podolská, K., (2022), Atmosphere 13(1), 13.
15. Alabdulgader, A., R. McCraty, M. Atkinson, et al., (2018), Scientific Reports} 8, 1–14
16. Palmer, S. J., M. J. Rycroft, M. Cermack, (2006), Surv. Geophys. 27, 557–593.
17. Georgiev, Ts. B., (2014), Bulg. Astron. J., 20, 14–25.
18. <https://www.nsi.bg/bg/content/2920/>
19. <https://omniweb.gsfc.nasa.gov/form/dx1.html>.
- [20] https://www.ngdc.noaa.gov>stp>geomag>kp_ap

ВЪРХУ ЗАКЪСНЕНИЕТО НА ДОПЪЛНИТЕЛНАТА СМЪРТНОСТ, СВЪРЗВАНА С ГЕОМАГНИТНИТЕ СМУЩЕНИЯ

Ц. Георгиев, С. Симеонова, Л. Данкова

Резюме

Геомагнитните смущения, главно геомагнитни бури (ГМБи), но и нискочестотни резонанси, засягат част от хората, предразположени към мозъчни и съдови болести (МСБи). Понякога геомагнитният ефект се надценява спекулативно. Срещу това ние сравняваме изменения на геомагнитни индекси (ГМИи) и изменения на добавъчна смъртност (ДС). Ние правим това чрез кроскорелационни функции (ККФи), използвайки числото на Волф (ЧВ) за референтна времева скала. Ние подозираме, че силни ГМБи, като тези през 2003 г., увеличават 3–4 г. по-късно относителната обща смъртност с до 4×10^{-5} . Иначе, типичната ДС, свързвана с ГМБи, е под $\sim 10^{-5}$ годишно. Даже ако тези наши величини са преувеличени, общо взето те са малки. Анализирайки данни за България и 5 нейни региони за последните 3 слънчеви цикли, ние потвърждаваме, че максимумът на ДС, свързвана с ГМБ, закъснява след максимума на ЧВ с ~ 5 г. Ние потвърждаваме и че максимумът на ГМБ закъснява след максимума на ЧВ с 1–2 г. Ние намираме специално, че максимумът на ДС, свързвана с ГМБи, закъснява след максимума на ГМИи с 3–4 г. По принцип, типичните продължителности на МСБи могат да бъдат определени, ако началата им са известни. В медицината началата са обикновено неизвестни. Обаче, подозирайки, че ГМБ са тригери на част от МСБи, ние следва да предположим, че тези МСБи завършват с летален изход след 3–4 г.